P3

Publication 3

P. Manninen, J. Hovila, P. Kärhä, and E. Ikonen, "Method for analysing luminous intensity of light-emitting diodes," *Meas. Sci. Technol.* Vol. **18**, No. 1, 223–229 (2007).

INSTITUTE OF PHYSICS PUBLISHING MEASUREMENT SCIENCE AND TECHNOLOGY

Meas. Sci. Technol. **18** (2007) 223–229 doi:10.1088/0957-0233/18/1/028

Method for analysing luminous intensity of light-emitting diodes

P Manninen[1], J Hovila[1], P Kärhä[1] and E Ikonen[1,2]

[1] Metrology Research Institute, Helsinki University of Technology (TKK), PO Box 3000, FI-02015 TKK, Finland

[2] Centre for Metrology and Accreditation (MIKES), PO Box 9, FI-02151 Espoo, Finland

E-mail: pasi.manninen@tkk.fi

Received 25 September 2006, in final form 8 November 2006
Published 7 December 2006
Online at stacks.iop.org/MST/18/223

Abstract

Light-emitting diodes (LEDs) have built-in lenses that enable spatially limited light beams. The use of lenses increases the luminous intensity levels, but complicates accurate LED intensity measurements. A novel method for determining the luminous intensity of the LED is proposed. The method based on a modified inverse-square law describes the behaviour of an LED in terms of its luminous intensity, the radius of the virtual source and the location of the virtual source. The applicability of the method was tested for 17 LED types with different packages, angular intensity distributions and power levels. When applying the new method to the measurement data, instead of the inverse-square law of the point source, the distance dependence of apparent LED luminous intensity of up to 47% reduced to statistical variation of less than 1%.

Keywords: light-emitting diodes, photometry, lenses, inverse-square law

(Some figures in this article are in colour only in the electronic version)

1. Introduction

Light-emitting diodes (LEDs) have become more and more popular light sources in several applications such as displays, banners, traffic lights, maritime signal lights, plant growth, general illumination and automotive headlights. The extensive application field of LEDs has created a need for high-accuracy LED characterizations. LEDs are found to have quasi-monochromatic spectra, diverse radiation patterns [1] and fairly stable light outputs [2, 3]. Differences of spatial and spectral features between LEDs and traditional light sources have increased the need to develop new measurement and analysis methods [4, 5]. This need is emphasized by the recently introduced high-intensity, narrow-beam LEDs.

Because of the high refractive index of the light-emitting layer of an LED, the majority of the light generated in the luminescent layer is trapped inside the semiconductor due to the total internal reflections on the LED–air boundary. Several solutions have been developed to overcome this problem. The enhancement of the coupling efficiency of the LED modifies the geometry of the light beam [6–8]. Furthermore, encapsulation of the LED, which not only provides mechanical protection but also acts as a lens, is used to get the desired light output [9].

LED manufacturers generally specify one single luminous intensity value in the specification of LEDs. However, luminous intensity measurements of the new LED types are problematic because the LEDs cannot necessarily be considered as point sources. Problems are encountered when the lens structure forms a virtual image of the LED source [10]. In that case, it is difficult to know exactly the size and location of the virtual source [11]. As a consequence, the specified luminous intensity value does not necessarily describe the photometric behaviour of the LED at varying distances. Calculating illuminance levels from the specified luminous intensity values may lead to errors of up to tens of per cent in, e.g., luminaire design. Low power levels of LEDs and discrepancies up to a few degrees [12] between their mechanical symmetry axis and optical axis also complicate the LED luminous intensity characterization. The mechanical axis of the LED is generally used as the measurement axis in the LED luminous intensity measurements.

In [11, 13], a couple of methods have been presented for measuring the position of the LED source to determine a

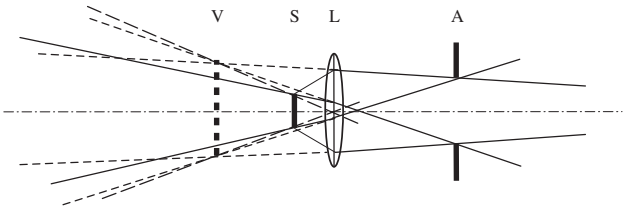

Figure 1. A two-aperture approximation of the LED measurement. The LED source containing lens is replaced by its virtual image. Note that in the figure the virtual source is located behind the front tip of the LED ($\Delta d_S > 0$). Abbreviations: V, virtual image source; S, LED source; L, lens; A, entrance aperture of photometer.

reliable luminous intensity value of the LED. However, these methods necessitate that the exact radius of the emitting area of the LED is known. Reference [14] recommends the distances to be measured from the front tip of the LED.

In this paper, the luminous intensities $I_{v,tip}$ and $I_{v,chip}$ of LEDs were determined at various distances d using two reference planes for the LED, the front tip of the LED ($\Delta d = 0$) and the site of the LED chip ($\Delta d > 0$), respectively. The measured illuminance values $E_v(d)$ were first assumed to obey the inverse-square law of the point source and detector:

$$E_v(d) = \frac{I_{v,tip/chip}}{(d + \Delta d)^2}. \tag{1}$$

Clear distance dependence of the determined luminous intensity value occurred in the measurements with respect to both reference planes. To be able to predict illuminances at any distance, a new method based on a two-aperture approximation with an extended source and detector was developed and tested. In the method, the behaviour of the LED is described by its luminous intensity and radius and location of the effective virtual LED source. The distance dependence of the apparent LED luminous intensity is removed when using this method and also the reproducibility of the results is good. It is recommended that especially high-intensity, narrow-beam LEDs are measured at sufficiently large distance and aligned with respect to their optical axis. It is also concluded that for LEDs with relatively broad angular intensity distribution, a simplified version of the new analysis method can be used.

2. Materials and methods

2.1. Description of the method

Measuring the illuminance produced by an LED with a lens is analogous to an optical system where a lens is located between two apertures. In this case, one of the apertures, the light-emitting surface of the LED, is like a point source. The optical system can be reduced to an equivalent optical system of two apertures by replacing the LED source with its virtual image of different location and size [15]. Figure 1 describes the formation of an extended virtual source when located behind the outermost tip of the LED.

When the virtual source of the LED is approximated to be circular, homogeneous, centred in the optical axis of the measurement system, and parallel with the photometer entrance plane, which has a circular shape, ideally cosinusoidal angular responsivity and uniform spatial responsivity, the modified inverse-square law of the distance dependence of illuminance can be presented in the form [16]

$$E_v(d) = \frac{I_{v,eff}}{(d + \Delta d_S)^2 + r_S^2 + r_P^2} g(d), \tag{2}$$

where $I_{v,eff}$ is the effective luminous intensity of the extended LED virtual source on the measurement axis, $d + \Delta d_S$ is the physical distance between the virtual source of the LED and the aperture plane of the photometer, and r_S and r_P are the effective radii of the virtual source and photometer aperture, respectively. The offset Δd_S fixes the position of the virtual source of the LED with respect to the front tip of the LED used as the distance reference plane in the measurements. The multiplication factor g is close to unity, as it is given by [16]

$$g(d) = \frac{2}{1 + \left\{1 - 4r_S^2 r_P^2 \Big/ \left[(d + \Delta d_S)^2 + r_S^2 + r_P^2\right]^2\right\}^{1/2}}. \tag{3}$$

For a reliable measurement of the LED luminous intensity, illuminances are measured at different distances d_i from the LED covering the distance range of interest. The apparent luminous intensity $I_{v,eff,i}$ of the LED at d_i is determined using equation (2) when r_P is known. The values for the quantities Δd_S and r_S are obtained by minimizing the relative standard deviation of the $I_{v,eff,i}$ values. The effective luminous intensity $I_{v,eff}$ of the LED is then calculated as an average of $I_{v,eff,i}$ values. Furthermore, we assume that the spectral mismatch correction of the photometer [14] is sufficiently well known so that the illuminance values can be determined from the measured photometer signal.

Equation (2) assumes the virtual source of the LED to be a Lambertian radiator. However, the LED sources often have strong angular intensity dependence. An LED can be considered as a directional radiator, the angular intensity distribution of which is described as [17, 18]

$$I_v(\theta) = I_v(0^\circ) \cos^n(\theta). \tag{4}$$

The parameter n indicates the degree of the directivity of the LED, θ is the angle between the viewing direction and the optical axis of the LED and $I_v(0^\circ)$ is the luminous intensity of the LED at its optical axis.

The influence of the directivity parameter n on equation (2) can be estimated by considering energy transfer between infinitesimal radiator and detector elements and by integrating the derived integrand over the full emitting and receiving surfaces [19]. The calculation leads to an approximation where the radius parameters in equation (2) can be presented in the form

$$r_{S/P} = \frac{r_{S0/P0}}{2}\sqrt{3 + n}, \tag{5}$$

where r_{S0} and r_{P0} indicate the radius of the virtual source of the LED and the physical radius of the entrance aperture of the photometer, respectively. For an inhomogeneous intensity distribution on the virtual source, the calculation yields an effective radius parameter r_{S0}. Otherwise equation (2) remains unchanged. It should be noted that for an LED with large n, the value of r_S can be much larger than r_{S0} and that the same relation is valid between r_P and r_{P0}. The data analysis can be made using equation (5), instead of equations $r_S = r_{S0}$ and

Table 1. Specifications of the tested LEDs. l indicates the distance between the front tip of the LED and the LED source chip. Parameter $\theta_{1/2}$ indicates the half-value angle of the angular distribution of the LED (full width at half maximum).

LED	Product number	Type	l (mm)	$\theta_{1/2}$	Note
LED 1	TLPG5600	Sideview	2.5	160°	
LED 2	L-1553SR	Square	6.0	110°	
LED 3	L-934SRC-G	T1	2.3	50°	
LED 4	E1L33-3G0A	T1	2.7	20°	
LED 5	100059, Marl	T1	3.0	25°	
LED 6	E1L5E-SG1A	Oval	3.0	40°/60°	Elliptical beam
LED 7	110147, Marl	T1 3/4	4.0	30°	
LED 8	HLMP-CM30	T1 3/4	5.0	30°	
LED 9	HLMP-ED31	T1 3/4	4.0	30°	
LED 10	HLMP-CB30	T1 3/4	5.0	30°	
LED 11	TLGE183P	T1 3/4	5.5	6°	
LED 12	E1L51-YC1A	T1 3/4	5.5	8°	
LED 13	L-813ID	10 mm	9.5	50°	
LED 14	TLOH190P	10 mm	11	4°	
LED 15	Luxeon Star™	1 W	2.5	Batwing	Green
LED 16	Luxeon Star™	1 W	8.0	18°	Collimator, white
LED 17	Luxeon Star™	1 W	8.0	18°	Collimator, green

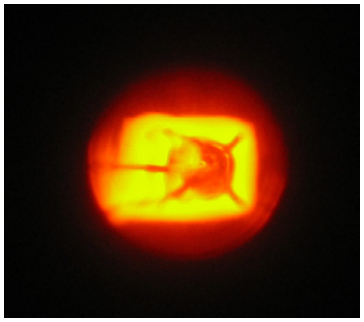

Figure 2. Photograph of the virtual image source of LED 14. The diameter of the outer circular area is 10 mm. The virtual source was photographed along the optical axis of the LED.

$r_P = r_{P0}$, in the fitting of the measured illuminance values using equation (2).

2.2. Photometer

As the photometer, a commercial LED standard photometer manufactured by LMT Lichtmesstechnik GmbH was used. The photometer has a circular entrance aperture with an area of 100 mm^2. The photometer has a planar diffuser behind the aperture to improve the angular responsivity of the photometer. The photometer was calibrated for the illuminance responsivity against the absolutely characterized reference photometer of the TKK [20]. For the determination of the spectral mismatch correction factor, the relative spectral responsivity of the photometer was measured with the reference spectrometer of the TKK [21].

2.3. Tested LEDs

The new method was tested with 17 different types of LEDs having a variety of packages, beam geometries and power levels. A brief summary of the specifications of the tested LEDs is presented in table 1. To illustrate the appearance of the LED virtual source, a photograph of LED 14 is shown in figure 2. The tested LEDs were mounted, one by one, on a specific holder made of PVC (polyvinyl chloride) and aluminium. There were two holes in the PVC part of the holder, where the leads of the LED were set. This enabled immovable conditions during the measurements and better repeatability of the results. Constant current of 330 mA was used for the high-power LEDs of 1 W and 20.0 mA for the other LEDs. Stability of the current setting was better than 0.02%.

2.4. Measurement set-up

The illuminance measurements were performed on a 4.5 m optical rail using a magnetic length measuring device with 0.1 mm resolution. Measurements were made at seven distances in various distance ranges depending on the power level of the tested LEDs. The luminous intensities of LEDs 3 to 15 were determined at a distance range of 200–800 mm and those of LEDs 16 and 17 at a range of 400–3000 mm due to their high power level. Illuminances of LEDs 1 and 2 were measured with 50 mm intervals between 50 mm and 350 mm because of their low power levels. The data analysis was performed with equations (1)–(5).

The photometer was mounted on a rail carrier and the tested LEDs were placed, one by one, at the other end of the optical rail. The mechanical symmetry axis of the tested LED was aligned perpendicular to the receiving aperture of the photometer and to cross the centre point of the photometer aperture by using a two-beam alignment laser and an alignment mirror. To get the correct orientations for the tested LEDs, aluminium bodies with bore diameters of 6 mm and 12 mm were used for the LED alignments.

The angular intensity distributions of the tested LEDs were measured with a turntable. The detector used in these measurements has a small entrance aperture with a diameter of 3 mm. The rotation axis was aligned to cross the front tip of the LED. The angular distributions were measured at various distances with 1° intervals. The measured angular distributions were fitted to equation (4) within a range of a few degrees around the LED optical axis.

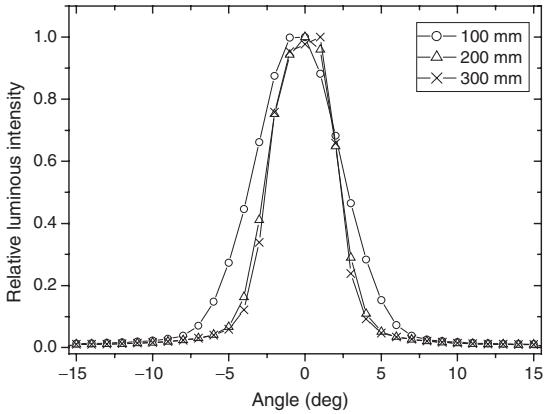

Figure 3. Angular distributions of LED 11 at three distances. The lines between data points guide the eye.

Table 2. Measurement results for the LEDs with moderate lenses. Parameter n is the degree of directivity of the LED. The quantities s_{chip} and s_{eff} indicate the relative standard deviation of the luminous intensities $I_{\mathrm{v,chip}}$ and $I_{\mathrm{v,eff}}$ determined at the measurement distances d with equations (1) and (2)–(5), respectively.

LED	n	$I_{\mathrm{v,eff}}$ (cd)	Δd_{S} (mm)	r_{S0} (mm)	s_{eff} (%)	s_{chip} (%)
LED 1	0.4	0.004	4.0	0.0	0.92	2.40
LED 2	1	0.003	−1.1	0.0	0.88	8.57
LED 3	8	1.3	2.4	0.0	0.09	0.12
LED 4	45	3.6	5.3	0.0	0.07	0.86
LED 5	29	3.7	3.4	0.0	0.39	0.42
LED 8	20	2.5	13.2	0.1	0.04	2.31
LED 15	1	5.6	3.0	0.0	0.05	0.10

The data acquisition and analysis were carried out with LabVIEW software. A digital voltmeter was connected to a measurement computer via the IEEE-488 bus. Dark current was measured before the signal measurements utilizing an electronic shutter controlled through the serial bus.

3. Measurement results

The measured angular distribution curves of LED 11 at three distances are presented in figure 3. The results from the illuminance measurements for the LEDs with moderate lenses and more powerful lenses are presented in tables 2 and 3, respectively. The LEDs with $r_{\mathrm{S0}} \leqslant 0.1$ mm are defined to have moderate lenses whereas the LEDs with larger r_{S0} have powerful lenses. The comparison of the results between the luminous intensities $I_{\mathrm{v,tip}}$, $I_{\mathrm{v,chip}}$ and $I_{\mathrm{v,eff}}$ as a function of the distance for LEDs 17 ($\Delta d_{\mathrm{S}} > 0$) and 14 ($\Delta d_{\mathrm{S}} < 0$) is shown in figures 4(*a*) and (*b*), respectively.

To investigate the reproducibility of the results, the measurement procedure was repeated a few times for some of the tested LEDs (LEDs 3, 10, 12, 16 and 17). Fairly reproducible luminous intensity values were obtained for these LEDs, the relative standard deviation being less than 1% for narrow-beam LEDs 11 and 12, and less than 0.3% for other LEDs. The values of the parameters Δd_{S} and r_{S} were reproduced typically with standard deviations of 5 mm and 0.5 mm, respectively. For LED 3, the corresponding values were 0.3 mm and 0.1 mm. The modified inverse-square law

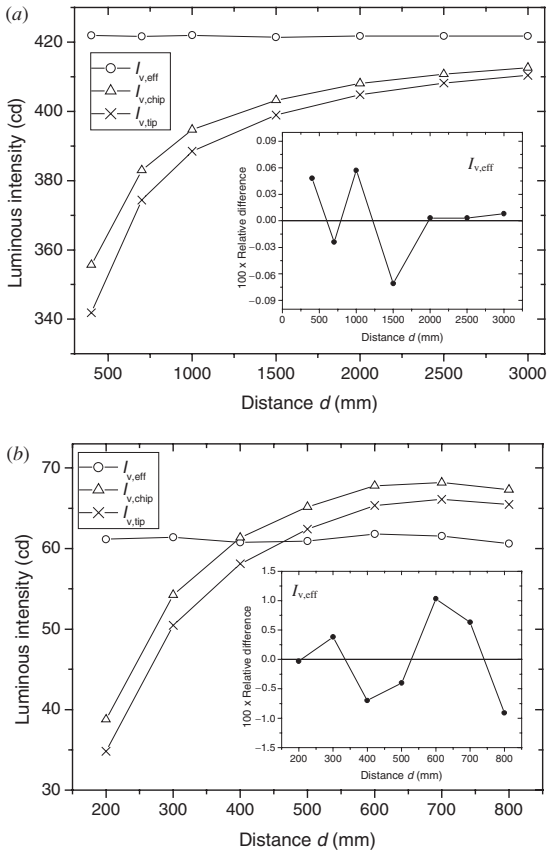

Figure 4. Luminous intensities $I_{\mathrm{v,tip}}$, $I_{\mathrm{v,chip}}$ and $I_{\mathrm{v,eff}}$ as a function of the distance for (*a*) LED 17 and (b) LED 14. The insets show the relative deviation of the luminous intensity $I_{\mathrm{v,eff}}$ of the LEDs at different distances.

Table 3. Measurement results for the LEDs with powerful lenses. Parameter n is the degree of directivity of the LED. The quantities s_{chip} and s_{eff} indicate the relative standard deviation of the luminous intensities $I_{\mathrm{v,chip}}$ and $I_{\mathrm{v,eff}}$ determined at the measurement distances d with equations (1) and (2)–(5), respectively.

LED	n	$I_{\mathrm{v,eff}}$ (cd)	Δd_{S} (mm)	r_{S0} (mm)	s_{eff} (%)	s_{chip} (%)
LED 6	7	1.8	0.9	0.9	0.26	0.40
LED 7	23	1.8	3.0	2.8	0.05	0.63
LED 9	20	3.2	7.6	1.0	0.07	1.33
LED 10	28	0.8	3.8	9.8	0.03	2.18
LED 11	810	9.0	−45.0	3.5	0.24	5.15
LED 12	590	11.7	−5.4	5.0	0.13	2.04
LED 13	15	4.7	4.8	7.8	0.05	1.70
LED 14	1915	61.2	−73.0	10.2	0.71	18.0
LED 16	73	287	−7.6	6.0	0.03	2.18
LED 17	85	422	40.5	11.6	0.06	4.70

fitting could be successfully carried out for each repetition measurement.

The cosine error of the photometer used was less than 0.01% at a distance of 200 mm and it decreases due to the smaller acceptance angle of the receiving aperture as the measurement distance increases (the largest acceptance angle was 6° for LEDs 13 and 14). Thus, the influence of the deviation between the angular response of the photometer and the ideal cosine response curve on the analysis is negligible.

Table 4. Deviations of the parameter values of table 3 for LEDs 12 and 14 from the values obtained when the measurement results were fitted with a fixed value of either n or g: $g = g(d)$, $n = 1$ or $g = 1$, $n = n$. Differences have been calculated by subtracting the value of table 3 from the new value of the parameter.

		$I_{v,eff}$			Δd_S			r_{S0}		
			Relative difference			Difference (mm)			Difference (mm)	
LED	n	Value (cd)	$g = g(d)$, $n = 1$	$g = 1$, $n = n$	Value (mm)	$g = g(d)$, $n = 1$	$g = 1$, $n = n$	Value (mm)	$g = g(d)$, $n = 1$	$g = 1$, $n = n$
LED 12	590	11.7	1.9%	1.9%	−5.4	1.6	1.6	5.0	81.6	−0.6
LED 14	1915	61.2	4.5%	4.6%	−73.0	27.3	27.4	10.2	212	−1.7

4. Discussion

4.1. Interpretation of source parameters

The data analysis according to section 2.1 for the LEDs of table 2 gives approximately zero for the value of r_{S0}. This indicates that these LEDs are well represented by a point source. For some LEDs, the point source appears to be located at the site of the LED chip. The inverse-square law for measuring luminous intensity works best for LEDs with moderate lenses. The LEDs of table 3 cannot be considered as point sources. The values of Δd_S and r_{S0} for these LEDs may differ significantly from the physical dimensions of the LED. They should thus be considered merely as parameters in the two-aperture approximation of the optical system.

Figures 4(*a*) and (*b*) indicate that the point-source and point-detector approximation for the LEDs with powerful lenses does not work very well. For the LEDs with negative Δd_S (see the denominator of equation (2)), there can be narrow distance ranges, where either the luminous intensity $I_{v,chip}$ or $I_{v,tip}$ matches the luminous intensity $I_{v,eff}$. By using the new method for the data analysis, the distance dependence of apparent LED luminous intensity of LEDs 17 and 14 of up to 17% and 47% is reduced to statistical variation (standard deviation) of 0.06% and 0.71%, respectively. For the luminous intensities $I_{v,chip}$ and $I_{v,tip}$, the distance dependence is defined as the relative difference between the minimum and maximum values. Once determined, Δd_S and r_{S0} can be used with $I_{v,eff}$ to calculate the illuminance at any distance from the LED.

For some LEDs of table 3, the virtual source was surprisingly large and located far either behind or in front of the outermost tip of the LED. This is due to different curvatures of the front tip of the LED packages and different distances between the source and the surface of the LED package. It is also noteworthy that the size and location of the LED virtual source for different colours of the same type of light sources (Luxeon Star LEDs 16 and 17) differed from each other quite a lot although the LEDs had similar collimation lenses. The effective source parameters seem to be very sensitive to small variations in manufacturing, such as dislocation of the LED package.

4.2. Applicability of the proposed method

To compare the results with those obtained by other analysis methods, the luminous intensities $I_{LED\,A}$ and $I_{LED\,B}$ defined by the CIE (Commission Internationale de l'Eclairage) [14] were determined. The ratios $I_{LED\,A}/I_{LED\,B}$ calculated for the tested LEDs varied from 0.25 to 3.96 [22]. Thus, the method proposed here gives significantly more consistent results, although it is somewhat more complicated than the method recommended by the CIE.

To determine the influence of the parameters g and n on the modified inverse-square law fitting, the analysis described in section 2.1 was repeated assuming first that $n = 1$ and then that $g = 1$. The tests were made with LEDs 12 and 14, because their values of the directivity parameter n were quite large. The values of the parameter $g(d)$ in equation (2) were 1.008 and 1.153 for these LEDs, calculated with the values of table 3 at a distance of 200 mm. The values approach 1, as the measurement distance d increases (see equation (3)). It can be noted from table 4 that the parameters n and g influence significantly the luminous intensity results of these LEDs. The large change of the parameter r_{S0} in the fit with $n = 1$ is explained by equation (5) and the tendency of the fitting to keep the squared sum $r_S^2 + r_P^2$ unchanged in equation (2). On the basis of table 4 and equations (2) and (5), it is easy to deduce that the influence of the parameters n and g on the determined luminous intensity becomes smaller as the value of n decreases.

It is of interest to determine such a value of the directivity parameter n, below which the luminous intensity analysis could be made reliably, although the effect of parameters n and g is omitted in equations (2) and (5), i.e., the fixed values $n = g = 1$ are used. Thus, simulated illuminance values were calculated in the distance range 200–800 mm using equations (2), (3) and (5) with the directivity parameter $n = 200$ and typical values $r_{S0} = 2$ mm and $\Delta d_S = 10$ mm. The simulated illuminance values were then used in the analysis where it was assumed that $g = 1$ and $n = 1$. Compared to the initial values, the obtained values for $I_{v,eff}$, Δd_S and $\sqrt{r_S^2 + r_P^2}$ changed by 0.005%, 0.03 mm and −0.20 mm, respectively.

It is concluded that the data analysis with $g = 1$ and $n = 1$ can be made with good accuracy at the studied distance range for LEDs with the value of n less than 200. If the LED has an angular luminous intensity distribution like $\cos^n(\theta)$, then $n = 200$ corresponds approximately to a half-value angle $\theta_{1/2}$ of 10° (full width at half maximum). This quantity is often specified in the LED datasheet and, with the known value of $\theta_{1/2}$, an LED user can decide relatively easily the necessity of the use of the parameters g and n in the luminous intensity analysis of the LED. In addition, in the illumination applications of high-brightness, narrow-beam LEDs, the viewer is typically in the far field of radiation, where the luminous intensity of the LED should also be determined. At large distances, the luminous intensity analysis with the use of equations $g = 1$ and $n = 1$ might be performed quite accurately regardless of the value of n.

To confirm the unambiguity of the solution in the modified inverse-square law fitting, the shape of the squared deviation surface was studied as a function of r_{S0} and Δd_S. The surface was smooth over all ranges and its gradient only had one zero. Thus, there was a global minimum which resulted in a unique solution (values of r_{S0} and Δd_S) for any measurement.

4.3. Choosing a reasonable measurement distance range

To measure the reliable luminous intensity of the LED, the angular width of the light beam of the LED should stay almost constant throughout the whole measurement range. Strong dependence of the angular distributions on distance occurred for several LEDs as shown in figure 3. However, this dependence only occurs with near field radiation. Farther from the LED, its angular intensity distribution is fixed as well as the luminous intensity of the LED. Thus, the luminous intensity, especially for high-intensity, narrow-beam LEDs, should be determined at sufficiently large distances. In the angular distributions of the tested LEDs, there were often specific fine structures and sidebands, which somewhat complicated the analysis of the measurement results.

The effect of selecting the distance range was investigated in the far field of radiation for two high-power LEDs (LEDs 16 and 17). These LEDs were measured at 11 distances within a distance range of 400–3000 mm and the analysis was performed at three narrower distance ranges. The studied ranges were 400–800 mm, 700–1500 mm and 1000–3000 mm. The standard deviations of the values of $I_{v,eff}$, Δd_S and r_{S0} obtained from these measurement ranges for LED 17 were 0.6%, 2.7 mm and 1.0 mm, respectively. This is within the reproducibility of the measurement results on the whole studied distance range. Thus, the parameter values determined for a certain distance range in the far field may also be utilized elsewhere in the far field of LED radiation.

4.4. Measurements with respect to the optical symmetry axis of LEDs

The reproducibility of the parameters was also studied by measurements where the LED was aligned with respect to its optical axis. The optical axis was found by maximizing the signal of the photometer at two distances. The influence of the measurement axis on the results was studied by rotating the LED around both its mechanical and optical symmetry axes with 90° steps and by measuring the LED parameters at each orientation. The measurements with respect to the optical axis of the LED gave more reproducible results for all kind of LEDs than the measurements with respect to the mechanical symmetry axis, the reproducibility of the parameters $I_{v,eff}$, Δd_S and r_{S0} being, for LED 11, 1.5%, 6.2 mm and 0.5 mm in the case of the optical axis and 7.4%, 14 mm and 2.0 mm in the case of the mechanical axis, respectively. This is understandable because small alignment errors, when aligning with respect to the mechanical axis, cause larger deviation in the intensity level than in the case of the optical axis. This holds up especially for narrow-beam LEDs [12]. When measuring such an LED, the luminous intensity value measured at the mechanical axis differed by as much as 50% from the value obtained at the optical symmetry axis of the LED beam. This is quite a large error for instance when designing the headlamp of a vehicle based on the LED sources. In future, it might be convenient to determine the luminous intensity of the LED with respect to the optical axis especially in the measurement laboratories, but it does not necessarily make sense to do this in field conditions. The alignment of narrow-beam LEDs could be done in a straightforward way by directing the light beam into the receiving aperture of the photometer at two distances.

5. Conclusions

A novel method for the determination of the luminous intensity of LEDs is described. The method based on the modified inverse-square law models the distance dependence of LED illuminance in terms of its luminous intensity, and the size and location of the apparent source. Many of the tested LEDs included a lens which complicated the luminous intensity measurements and analysis. However, the lens effect could be removed by returning the optical system to a two-aperture approximation with the virtual source of the LED and the receiving aperture of the photometer. Applicability of the method has been demonstrated with 17 different LED types, for which the luminous intensities according to the point-source and point-detector approximation were also determined. When applying the new method to the measurement data, the distance dependence of apparent LED luminous intensity of up to 47% reduced to statistical variation of less than 1%.

Significant simplification of the new method could be achieved when analysing LEDs with broad beams. When the half-width angle is larger than 10°, the luminous intensity of the LED can be determined sufficiently accurately without detailed information on the angular intensity distribution.

When determining the luminous intensities of LEDs, the measurement ranges should be selected depending on the application. For example, high-power LEDs are typically used in applications where the viewer is far away from the light source. Therefore, the luminous intensity measurements would be convenient to perform at large distances.

Reproducibility of the luminous intensity values for all tested LEDs was better than 1%. It was also noted that when the illuminance measurements are made with respect to the optical axis of the LED, it enables better reproducibility of the measurement results for the LEDs with spatially non-uniform light beams.

The method gave notably consistent results for the standard deviation of the luminous intensities measured at different distances being less than 0.3% for most of the tested LEDs. For instance, LED manufacturers could measure and specify luminous intensity values for their LEDs with the new method. Designers of LED luminaires could then use the published values to estimate more accurately the photometric behaviour of the light systems being designed before building prototypes. This would reduce the need to overdesign illuminance levels and the number of prototype cycles.

Acknowledgments

PM would like to acknowledge grants from the Jenny and Antti Wihuri Foundation, the Finnish Cultural

Foundation and the Research Foundation of Helsinki University of Technology.

References

[1] Sauter G 1991 *Metrologia* **28** 239–42
[2] Benavides J M and Webb R H 2005 *Appl. Opt.* **44** 4000–3
[3] Agaphonov D R, Ivanov V S, Sapritsky V I and Stolyarevskaya R I 2000 *Metrologia* **37** 587–90
[4] Ohno Y 2006 *Proc. SPIE* **6046** 604625
[5] Godo K, Saito T, Shitomi H, Zama T and Saito I 2005 *Proc. NEWRAD2005*, p 199. Available online at http://www.pmodwrc.ch/newrad2005/pdfabstracts/Newrad095.pdf
[6] Cuong T V, Cheong H S and Hong C-H 2004 *Phys. Status Solidi* C **1** 2433–7
[7] Madigan C F, Lu M H and Sturm J C 2000 *Appl. Phys. Lett.* **76** 1650–2
[8] Luo H, Kim J K, Schubert E F, Cho J, Sone C and Park Y 2005 *Appl. Phys. Lett.* **86** 243505
[9] Norris A W, Bahadur M and Yoshitake M 2005 *Proc. SPIE* **5941** 207–13
[10] Gillies G T 1980 *Am. J. Phys.* **48** 418–9
[11] Muray K 1991 *Appl. Opt.* **30** 2178–86
[12] Bürmen M, Pernuš F and Likar B 2006 *Meas. Sci. Technol.* **17** 1372–8
[13] Muray K 1988 *Proc. Soc. Photo-opt.* **954** 560–7
[14] Commission Internationale de l'Eclairage 2003 *CIE Publication* 127.2
[15] Nicodemus F E 1979 *Self-Study Manual on Optical Radiation Measurements* (Washington, DC: National Bureau of Standards) pp 91–119
[16] Walsh J W T 1965 *Photometry* (New York: Dover) pp 120–73
[17] Altendorf E 2003 *Proc. SPIE* **4996** 208–20
[18] Sauter G 2001 *2nd CIE Expert Symp. on LED Measurement* (presentation)
[19] Ikonen E, Manninen P, Hovila J and Kärhä P 2006 *Proc. Metrology Symp. (Queretaro)* (CD, 5 pp)
[20] Toivanen P, Kärhä P, Manoochehri F and Ikonen E 2000 *Metrologia* **37** 131–40
[21] Manoochehri F, Kärhä P, Palva L, Toivanen P, Haapalinna A and Ikonen E 1999 *Anal. Chim. Acta* **380** 327–37
[22] Kärhä P, Manninen P, Hovila J, Seppälä L and Ikonen E 2005 *Proc. NEWRAD2005* pp 211–2 Available online at http://www.pmodwrc.ch/newrad2005/pdfabstracts/Newrad044.pdf